J. Geogr. Sci. 2014, 24(1): 93-112
DOI: 10.1007/s11442-014-1075-5

Quantitative estimation of climate change effects on potential evapotranspiration in Beijing during 1951–2010

LIU Haijun[1,4], LI Yan[1,2], JOSEF Tanny[3], ZHANG Ruihao[1], HUANG Guanhua[2]

1. College of Water Sciences, Beijing Normal University, Beijing 100875, China;
2. College of Water Resources and Civil Engineering, China Agricultural University, Beijing 100083, China;
3. Institute of Soil, Water and Environmental Sciences, Agricultural Research Organization, The Volcani Center, P. O. Box 6, Bet Dagan 50250, Israel;
4. State Key Laboratory of Simulation and Regulation of Water Cycle in River Basin, China Institute of Water Resources and Hydropower Research, Beijing 100048, China

Abstract: Climate change is likely to affect hydrological cycle through precipitation, evapotranspiration, soil moisture etc. In the present study, an attempt has been made to study the climate change and the sensitivity of estimated evapotranspiration to each climatic variable for a semi-arid region of Beijing in North China using data set from 1951 to 2010. Penman-Monteith method was used to calculate reference crop evapotranspiration (ETo). Changes of ETo to each climatic variable was estimated using a sensitivity analysis method proposed in this study. Results show that in the past 60 years, mean temperature and vapor pressure deficit (VPD) were significantly increasing, relative humidity and sunshine hours were significantly decreasing, and wind speed greatly oscillated without a significant trend. Total precipitation was significantly decreasing in corn season (from June to September), but it was increasing in wheat season (from October to next May). The change rates of temperature, relative humidity, VPD, wind speed, annual total precipitation, sunshine hours and solar radiation were 0.42℃, 1.47%, 0.04 kPa, 0.05 $m \cdot s^{-1}$, 25.0 mm, 74.0 hours and 90.7 $MJ \cdot m^{-2}$ per decade, respectively. In the past 60 years, yearly ETo was increasing with a rate of 19.5 mm per decade, and total ETos in wheat and corn seasons were increasing with rates of 13.1 and 5.3 mm per decade, respectively. Sensitivity analysis showed that mean air temperature was the first key factor for ETo change in the past 60 years, causing an annual total ETo increase of 7.4%, followed by relative humidity (5.5%) and sunshine hours (–3.1%); the less sensitivity factors were wind speed (0.7%), minimum temperature (–0.3%) and maximum temperature (–0.2%). A greater reduction of total ETo (12.3%) in the past 60 years was found in wheat season, mainly because of mean temperature (8.6%) and relative humidity (5.4%), as compared to a reduction of 6.0% in ETo during corn season due to sunshine

Received: 2012-11-12 **Accepted:** 2013-09-17
Foundation: Open Research Funds of State Key Laboratory of Simulation and Regulation of Water Cycle in River Basin, No.IWHR-SKL-201105; National Natural Science Foundation of China, No.51179005; Fundamental Research Funds for the Central Universities, No.2009SD-10
Author: Liu Haijun (1975–), PhD and Associate Professor, specialized in crop evapotranspiration and irrigation scheduling. E-mail: shanxilhj@bnu.edu.cn

hours (–6.9%), relative humidity (4.7%) and temperature (4.5%). Increasing precipitation in the wheat season will improve crop growth, while decreasing precipitation and increasing ETo in the corn season induces a great pressure for local government and farmers to use water more efficiently by widely adopting water-saving technologies in the future.

Keywords: climatic variables; reference crop evapotranspiration; Penman-Monteith equation; changing trend; sensitivity analysis

1 Introduction

It has been confirmed that there has been a change in earth climate, which is closely related to the increases in atmospheric greenhouse gases (CO_2, NO_x) concentrations and other radioactively active gases (IPCC, 2007). These changes in climate are expected to cause major changes in various climatic variables such as precipitation, air temperature, relative humidity, and solar radiation (Haskett *et al*., 2000). According to the IPCC report (IPCC, 2007), the air temperature at the earth surface level rose by 0.74℃ from 1906 to 2005, and this rising trend of air temperature is likely to continue in the 21st century, which will cause changes in the hydrological cycle by affecting precipitation and evaporation (Huntington, 2006; Bates *et al*., 2008). Bates *et al*. (2008) pointed out that, over the last century, precipitation has mostly increased over land in high northern latitudes, but decreased from 10°S to 30°N since the 1970s, and globally, the area of land classified as very dry has more than doubled since the 1970s due to climate change.

In a regional scale, climatic variables change from one place to another. Chaouche *et al*. (2010) found in French Mediterranean Region that, there were an increase in annual mean temperature and annual potential evapotranspiration, whereas annual precipitation has not exhibited any trend. In southern Spain, Espadafor *et al*. (2011) found trends of increased air temperature and solar radiation, and decreased relative humidity.

Any changes in meteorological variables due to climate change will affect evapotranspiration or crop water requirement, and eventually affect water allocation for agriculture and food production (Zhang *et al*., 2011). In recent years, numerous studies have been conducted to examine the potential impact of climate change on reference evapotranspiration (ETo). Espadafor *et al*. (2011) found a significant increase in ETo (up to 3.5 mm $year^{-1}$) in southern Spain and pointed out that this increase was mainly due to the increases in air temperature and solar radiation, and the decreases in relative humidity. Tabari *et al*. (2011) indicated in the western half of Iran, a significant positive trend in annual ETo varying from 11.28 to 2.30 mm $year^{-1}$, and stronger increasing trends in winter and summer compared with those in autumn and spring. They further pointed out that the significant increasing trend in ETo was mainly caused by a significant increase in air temperature. Chattopadhyay and Hulme (1997) showed that, both pan evaporation (Epan) and ETo have decreased during recent years (30 years) in India and they further pointed out that increases in relative humidity and decreases in radiation were the main reasons for the decreasing ETo. However, they modeled that future warming would likely lead to increased potential evapotranspiration over India.

In China the climate change effect on ETo has also been studied in regional and national scales. Tang *et al*. (2011) analyzed a potential evapotranspiration time series over 58 years in the Haihe River Basin of North China and showed that ETo gradually decreased in the whole basin at a rate of –1.0 mm $year^{-1}$. They attributed this finding to decreases of net radiation

(–0.9 mm·year^{-1}), vapour pressure (–0.5 mm·year^{-1}), wind speed (–1.3 mm·year^{-1}) and air temperature (–1.7 mm·year^{-1}). Liu and Yang (2010) studied the spatial distribution and temporal trends for potential evapotranspiration at 89 meteorological stations during 1961–2006 in the Yellow River Basin (YRB), China. They found a positive trend of ETo in the middle YRB, but the trends were negative in the upper, lower and whole YRB. Gong *et al*. (2006) and Wang *et al*. (2007) evaluated the spatial distribution and temporal trend of ETo and pan evaporation (Epan) in the Yangtze River Basin in China during 1960–2000, and found a significant decreasing trend in both ETo and Epan, which was mainly caused by a significant decrease in net total radiation and wind speed over the basin. The reductions of Epan and ETo during the summer months contributed the most to the total annual reduction of Epan and ETo in the Yangtze River Basin. Liang *et al*. (2006) reported that ETo showed an increasing tendency during 1951–2000 in west Songnen Plain in North China and found that decreasing humidity and increasing air temperature were the main reason for the increase in ETo (Liang *et al*., 2008). Thomas (2000) analyzed the climate data in China during 1954–1993, and showed that potential evapotranspiration has decreased in all seasons, especially in Northwest and Southeast China. Tao *et al*. (2003) analyzed the climatic variables and ETo changes in China under the HADCM2 climate-change scenarios, and found that the mean annual ETo during the 2020s is expected to decrease in up to 20 mm in South China and to increase in up to 20 mm in other regions. Liu *et al*. (2012) also found a decreasing trend of ETo in most regions of China, and pointed out that, at national scale, the most sensitive factors for ETo variation were vapor pressure deficit, maximum daily temperature, radiation and wind speed. A decreasing trend in ETo generally reduces agricultural water demand.

Beijing, the capital of China, is located in semi-humidity and semi-arid region in North China, and has been seriously suffering from water shortage. In the past 50 years, annual precipitation has gradually decreased (Yue, 2007). Consequently, irrigation is the base of food production in Beijing region. However, with the rapid growth in water demand due to growth of economy and urban population, water allocation for agriculture in Beijing has decreased dramatically over the past 30 years, from 3.183 billion m^3 in 1980 to 1.2 billion m^3 in 2009 (Beijing Water Resources Bulletin, 1980–2009). Consequently the sustainable development of agriculture as well as economy in Beijing is compromised. Water allocation for agriculture mainly depends on the precipitation and crop water requirement (ET). The crop ET is generally calculated using crop coefficient and ETo. Therefore, analyzing the trends of climate change and their effect on ETo is important for water resources management, and the sustainable development of agriculture and economy in Beijing. To our knowledge, there were only few comprehensive researches on the climate and ETo trend and the dominant climatic factors affecting ETo in Beijing, which in turn affect precisely estimating crop evapotranspiration and making water allocation for agriculture.

In this study, daily ETo in Beijing was calculated by Penman-Monteith method (Allen *et al*., 1998) using meteorological data sets from 1951 to 2010. We analyzed the trends of change of each measured meteorological variable (i.e. precipitation, air temperature, relative humidity, sunshine hours, wind speed, saturated vapor pressure deficit and solar radiation) and ETo, and analyzed the key factors influencing ETo using a sensitivity analysis method. Results from this paper are helpful for further study on climatic change and irrigation scheduling in Beijing Region.

2 Data and methods

2.1 Site

Beijing (39°28′–41°05′N, 115°25′–117°30′E), the capital of China, lies on the northern edge of the North China Plain (Figure 1). It is flanked on the north and west by the Jundu Mountain and Xishan (west) Mountain. The area administrated by the Beijing Municipal Government is 16,807 km^2, and 62% of which is hilly (Yang *et al.*, 2005). Beijing has a typical East Asian monsoon climate. In autumn, winter and spring (from October to May), the sky conditions are mostly clear, precipitation is low, humidity is low and wind speed is generally high. Summer is generally entitled as the “wet seasons”, in which humidity and precipitation are high and wind speed is low. Mean annual precipitation is 580 mm, about 70% distributed in summer, the rainy season. The annual mean temperature is 11.5℃, the minimum mean monthly temperature is –4.6℃ in January, and the maximum is 25.8℃ in July. Wheat-corn rotation system is the traditional cultivation practice in Beijing. With this system, the annual crop water requirement is 876 mm, 453 mm of which is for winter wheat and 423 mm for summer corn (Liu *et al*., 2002; Zhang *et al*., 2011).

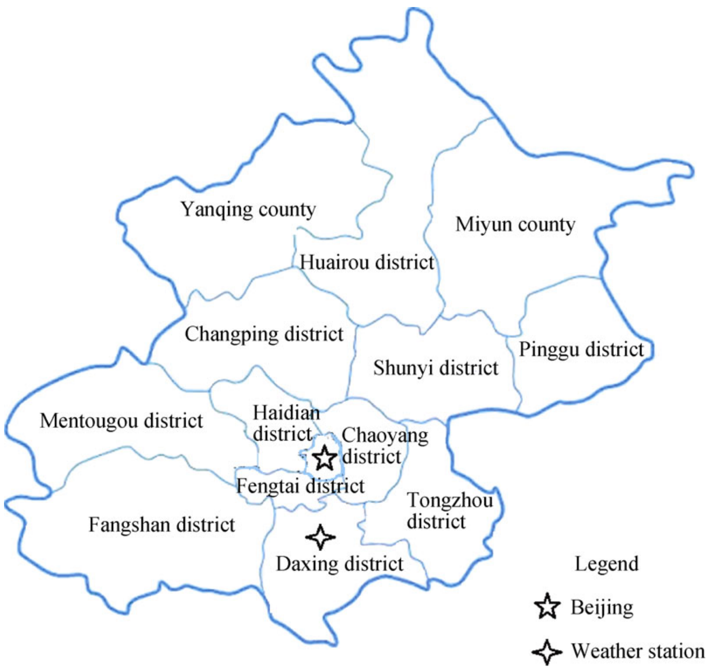

Figure 1 Schematic diagram of the research region (Beijing) and the meteorological station

2.2 Meteorological data

All meteorological data are from a national climatic station, located south of Beijing city (39°48′N, 116°28′E, 31.3 m above sea level) (Figure 1). The meteorological data include atmospheric pressure, daily values of precipitation, mean, maximum and minimum temperatures, mean relative humidity, mean wind speed, and sunshine hours from 1951 to 2010.

2.3 Methods

2.3.1 Reference crop evapotranspiration

Reference crop evapotranspiration (ETo) was calculated using FAO Penman-Monteith method (hereafter denoted as P-M). The P-M method is (Allen *et al.*, 1998):

$$ETo = \frac{0.408\Delta(R_n - G) + \gamma \frac{900}{(T+273)} U_2 (e_s - e_a)}{\Delta + \gamma(1 + 0.34U_2)} \tag{1}$$

where ETo is the reference crop evapotranspiration, mm·day^{-1}; R_n is the net radiation, MJ·m^{-2}·day^{-1}; G is the soil heat flux that can be neglected on daily intervals (Allen *et al.*, 1998), MJ·m^{-2}·day^{-1}; γ is the psychrometric constant, kPa·℃$^{-1}$; U_2 is the wind speed measured at 2 m above ground surface, m·s^{-1}; e_s and e_a are the saturation and the actual vapor pressure, kPa; and Δ is the slope of the saturation vapor pressure curve at air temperature, kPa·℃$^{-1}$.

Net radiation was not directly measured at Beijing station. Therefore net radiation was calculated using data of daily sunshine hours, and maximum and minimum air temperatures, following the method suggested by Allen *et al.* (1998). The daily net radiation is the difference between the daily incoming net short-wave radiation (R_{ns}, MJ·m^{-2}·day^{-1}) and the daily outgoing net long-wave radiation (R_{nl}, MJ·m^{-2}·day^{-1}):

$$R_n = R_{ns} - R_{nl} \tag{2}$$

The net short-wave radiation (R_{ns}) is calculated from the balance between incoming and reflected solar radiation, and is given by:

$$R_{ns} = (1 - \alpha) R_s \tag{3}$$

where

$$R_s = \left(a_s + b_s \frac{n}{N} \right) R_a , \tag{4}$$

α is the albedo or canopy reflection coefficient, given as 0.23 for the hypothetical grass reference crop (Allen *et al.*, 1998); R_s is the incoming solar radiation, MJ·m^{-2}·day^{-1}; n is actual daily sunshine duration, hours, which was measured in this study; N is the maximum possible duration of sunshine at Beijing station, hours; n/N represents the relative sunshine duration; R_a is extraterrestrial radiation, MJ·m^{-2}·day^{-1}; a_s is regression constant, expressing the fraction of extraterrestrial radiation reaching the earth on overcast days (n = 0) and "a_s+b_s" is the fraction of extraterrestrial radiation reaching the earth on clear days ($n = N$). The values of a_s and b_s depend on atmospheric conditions (humidity, dust) and solar declination (latitude and month). In this study, $a_s = 0.25$ and $b_s = 0.50$ following the recommendation of Allen *et al.* (1998).

The long-wave energy emission flux is proportional to the absolute temperature of the surface raised to the fourth power, and is also influenced by water vapor, clouds, carbon dioxide and dust. The latter absorb and emit long-wave radiation, especially under humid and cloudy conditions. The corrected Stefan-Boltzmann law for estimating the net outgoing flux of long-wave radiation is:

$$R_{nl} = \sigma\left(\frac{T_{\max,K}{}^4 + T_{\min,K}{}^4}{2}\right)\left(0.34 - 0.14\sqrt{e_a}\right)\left(1.35\frac{R_s}{R_{so}} - 0.35\right) \tag{5}$$

where R_{nl} is net outgoing long-wave radiation, MJ·m^{-2}·day^{-1}; σ=4.903×10^{-9} is Stefan-Boltzmann constant, MJ·K^{-4}·m^{-2}·day^{-1}; $T_{\max,K}$ is maximum absolute temperature during the 24-hour period, K; $T_{\min,K}$ is minimum absolute temperature during the 24-hour period, K; e_a is actual vapor pressure, kPa; R_s is the incoming solar radiation, MJ·m^{-2}·day^{-1} calculated using Eqn. (4). R_{so} is clear-sky radiation calculated as:

$$R_{so} = (0.75 + 2\times10^{-5} z)R_a \tag{6}$$

where z is station elevation above sea level, m. Extraterrestrial radiation (R_a) for each day of a year at the Beijing station was estimated following the procedure outlined in Allen *et al*. (1998).

Actual daily vapor pressure (e_a, kPa) and vapor pressure deficit (VPD, kPa) were based on daily mean temperature and relative humidity, and were calculated as:

$$e_a = RH \times e^o\left(T_{mean}\right) \tag{7}$$

and

$$VPD = \left(1 - RH\right) \times e^o(T_{mean}), \tag{8}$$

where RH is daily mean relative humidity, %; T_{mean} is daily mean temperature, ℃; and $e^o\left(T_{mean}\right)$ is saturated vapor pressure at T_{mean}, kPa. $e^o\left(T_{mean}\right)$ is calculated as follows:

$$e^o\left(T_{mean}\right) = 0.6108\exp\left(\frac{17.27T_{mean}}{T_{mean} + 237.3}\right). \tag{9}$$

2.3.2 Sensitivity analysis method

Sensitivity analysis was employed to identify the climatic variables that mostly influence ETo following the method proposed by Möller *et al*. (2004). The process of the sensitivity analysis is described as follows. (1) Calculating the mean values of air temperature, relative humidity, wind speed and sunshine hours in each day of a year using climatic data from 1951 to 1960 (referring to the 1950s), and estimating the corresponding daily ETo using the mean daily values during the 1950s. The mean daily value for each climatic variable in the 1950s was set as reference climatic variable, and the estimated daily ETo was set to the reference ETo. The same method was used to calculate mean value of each climatic variable of each day of a year using data in 2001–2010 (referring to the 2000s), and estimate the corresponding daily ETo. (2) Calculating ETos of each day of a year using the P-M method by setting one climatic variable to its respective data in the 2000s (i.e. the mean daily climatic variable in the period from 2001 to 2010) and others to their reference data (the mean daily value in the 1950s calculated in the step (1)). (3) Comparing the ETos calculated by replacing each variable using data in the 2000s (in the step (2)) with the reference ETo in the 1950s (in the step (1)) and find out the variables mostly influencing ETo.

2.3.3 Mann–Kendall test

Mann-Kendall test is one of the most widely used non-parametric tests to detect significant trends of climatic variables and potential evapotranspiration in time series (Hamed, 2008, Liang *et al*., 2010). The Mann-Kendall test is based on the statistic *S*:

$$S = \sum_{i=1}^{N-1} \sum_{j=i+1}^{N} \operatorname{sign}(x_j - x_i) \tag{10}$$

where x_i and x_j are two generic sequential data values of the variable, *N* is the length of the data set, and the sign (*X*) takes the following values:

$$\operatorname{sign}(X) = \begin{cases} +1 & \text{if} \quad X > 0 \\ 0 & \text{if} \quad X = 0 \\ -1 & \text{if} \quad X < 0 \end{cases} \tag{11}$$

A positive *S* in Eqn. (10) represents a positive trend in the observed data series, and vice versa. Under the null hypothesis of no trend in the data, H_0, the statistic S is approximately normally distributed with the mean E(S)=0. For data sets with more than 10 values, the variance associated with the Mann-Kendall statistic S (*VAR*(*S*)) can be calculated after considering the distribution as very close to normal:

$$VAR(S) = \frac{1}{18}\left[N(N-1)(2N+5) - \sum_{p=1}^{q} t_p (t_p - 1)(2t_p + 5) \right] \tag{12}$$

where *q* is the number of tied groups and t_p is the number of data values in the *p*th group.

The values of *S* and *VAR(S)* are used to compute the test statistic *Z* as follows

$$Z = \begin{cases} \dfrac{S-1}{\sqrt{VAR(S)}} & \text{if} \quad S > 0 \\ 0 & \text{if} \quad S = 0 \\ \dfrac{S+1}{\sqrt{VAR(S)}} & \text{if} \quad S < 0 \end{cases} \tag{13}$$

The presence of a statistically significant trend is evaluated using the *Z* value. A positive (negative) value of *Z* indicates an upward (downward) trend. The statistic *Z* has a normal distribution. To test for either an upward or downward monotone trend (a two-tailed test) at α level of significance, H_0 is rejected if the absolute value of *Z* is greater than $Z_{1-\alpha/2}$, where $Z1_{-\alpha/2}$ is obtained from the standard normal cumulative distribution tables. The tested significance levels, α, were set to 0.001, 0.01, 0.05 and 0.1 in this study.

2.3.4 Sen's slope estimator

If a linear trend is present in a time series, then the true slope (change per unit time) can be estimated using a simple nonparametric procedure given by Sen (1968). The Sen's slope estimator, *b*, is (Sen, 1968):

$$b = Median\left(\frac{x_j - x_i}{j-1} \right) \qquad \forall i < j \tag{14}$$

For a time series of annual (crop seasonal or monthly) values, *b* represents the annual (crop seasonal or monthly) increment under the hypothesis of a linear trend. This estimator gives the real slope of the tendency, which can slightly differ from the slope of the trend line obtained by linear regression.

The Mann-Kendall test and Sen's slope estimator calculation for monthly, seasonal and annual mean series of the meteorological variables and ETo values were done using the EXCEL-based software of MAKESENS 1.0 developed by Salmi *et al*. (2002).

3 Results and discussion

3.1 Monthly, seasonal and annual distributions of climatic variables and ETo

Monthly means or totals of climatic variables and reference crop evapotranspiration (ETo) averaged during period from1951 to 2010 are given in Figure 2. It can be seen from the figure that, most climatic variables showed a clear single peak curve in its annual distribution, except monthly sunshine hours. Generally, the highest temperature occurs during June and August (Figure 2c). The greatest precipitation in July and August (Figure 2b) causes higher relative humidity, which in turn results in relative low vapor pressure deficit (Figure 2e). The highest wind speed was found in April and the lowest one in August (Figure 2f). Monthly totals of sunshine hours and solar radiation showed similar annual distributions except in July and August (Figures 2g and 2h). The low value of sunshine hours in July and August is mainly due to great number of cloudy and rainy days. This can be confirmed by greater precipitation amount in July and August in Figure 2b. The higher solar radiation amount (Figure 2h) in July and August may be mainly due to higher density of solar radiation in this period (Figure 3). The solar radiation densities of 2.8 and 2.7 $MJ \cdot m^{-2} \cdot h^{-1}$ in July and August not only compensate the reduction of radiation amount caused by low sunshine hours, but further increase the radiation amount, which finally result in a single peak curve of radiation amount in a year course. Monthly ETo, comprehensively influenced by all climatic variables, also showed a single peak curve (Figure 2a). The peak values were in May (160.6 mm) and June (160.9 mm) and the smallest value was found in December (32.8 mm).

In Beijing region, winter wheat/summer corn rotation system is the main agricultural practice. Winter wheat season is generally from the October to the middle June, and the summer corn seasons is from middle June to end of September. Crop seasonal (winter wheat season and summer corn season) and annual means or totals of climatic variables and ETo from 1951 to 2010 are given in Table 1. As shown in Table 1, total precipitation in the wheat season was 122 mm, which was much less than the 439 mm of the summer season. The reference crop evaporations in the wheat and corn seasons were 665 and 439 mm, respectively. Using a crop coefficient of 0.85 for winter wheat and 0.94 for summer corn in the North China Plain (Zhang *et al*., 2011), the seasonal water requirements are 532 mm for wheat and 395 mm for corn. Comparing to the seasonal precipitation, more than 400 mm would be applied to wheat as irrigation. Though total precipitation can meet water requirement of corn, corn is always irrigated once or twice due to non-matching distributions of rain and water requirement in the corn season, especially during the initial period of corn season, from late June to middle July. In fact, real crop evapotranspiration is less than the above estimated water requirements for both wheat (532 mm) and corn (395 mm), mainly because of wide applications of various water-saving technologies and deficit irrigation scheduling (Liu and

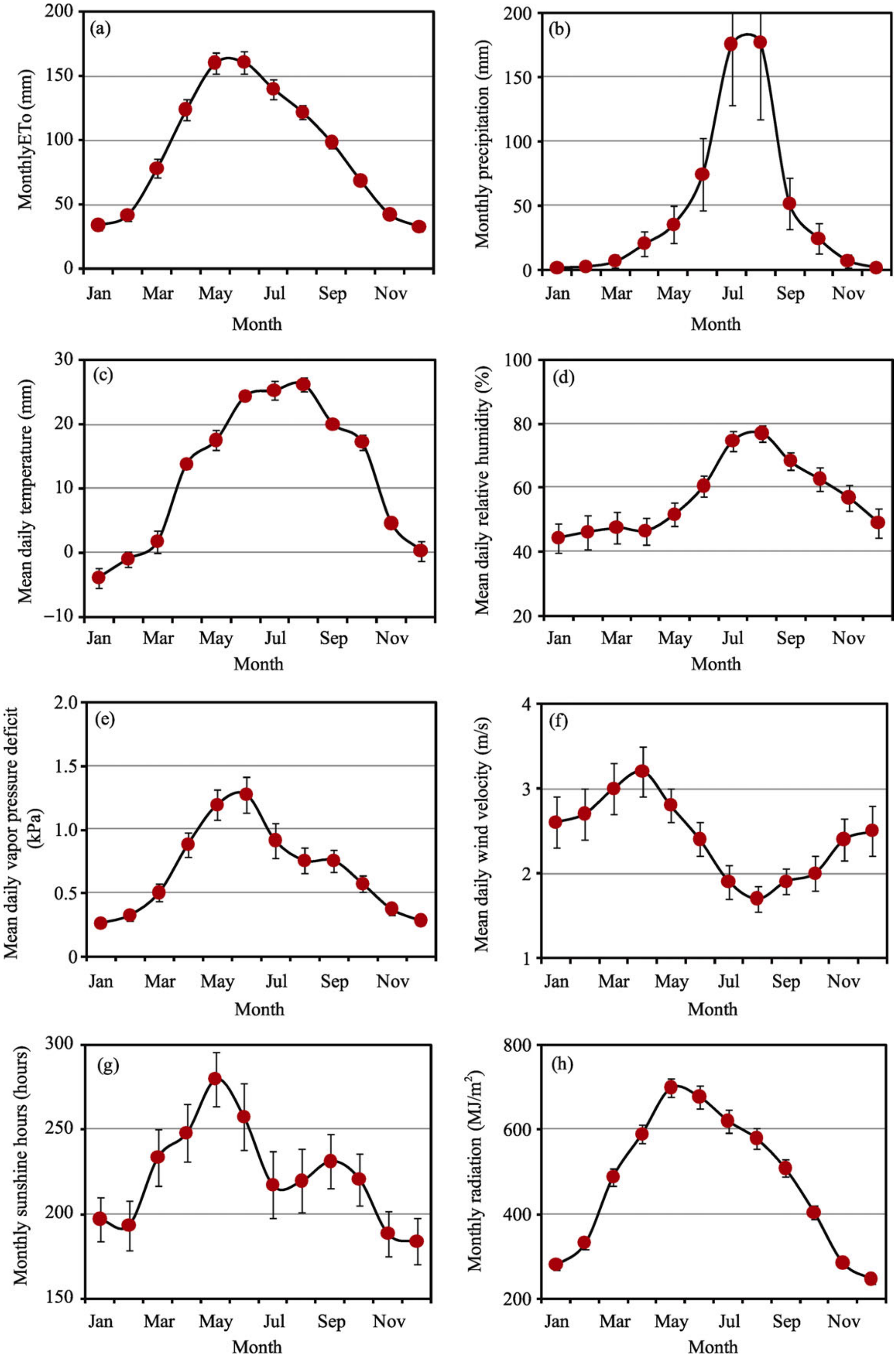

Figure 2 Yearly variations of ETo (a), precipitation (b), temperature (c), relative humidity (d), vapor pressure deficit (e), wind velocity (f), sunshine hours (g) and radiation amount (h) averaged from 1951 to 2010

Table 1 Reference evapotranspiration (ETo) and climatic variables (daily temperature, relative humidity, vapor pressure deficit VPD, wind speed, sunshine duration and solar radiation) at seasonal (wheat and corn) and annual scales in Beijing, 1951–2010

Period	Variable							
	Total ETo	Total precipitation	Mean T	Mean RH	Mean VPD	Mean wind	Total sunshine hours	Total solar radiation
	mm	mm	℃	%	kPa	$m \cdot s^{-1}$	Hours	$MJ \cdot m^{-2}$
Wheat season (Oct. 1 to Jun. 15)	665±50	122±60	7.3±1.0	50.8±4.8	0.59±0.09	2.6±0.4	1878±130	3660±144
Corn season (Jun. 16 to Sep. 30)	439±33	439±161	24.0±0.9	72.0±4.7	0.86±0.19	1.9±0.3	787±100	2031±135
Annual	1105±37	577±202	12.2±0.9	57.0±4.2	0.67±0.11	2.4±0.3	2674±203	5705±250

Kang, 2007; Liu *et al.*, 2011).

3.2 Trends of climatic variables and ETo

Figure 4 describes the changing trend of mean temperature, relative humidity, vapor pressure deficit, wind speed, total annual sunshine hours, radiation, precipitation and ETo from 1951 to 2010 in Beijing region. Sen's rates of the linear slopes for each climatic variable and ETo and the corresponding statistical test on the linear change rate using Mann-Kendall test are listed in Table 2. It can be found in Figure 4a that, air temperature, including annual and seasonal mean temperatures, increased from 1951 to 2010. The mean temperature increased by 1.91℃, 1.63℃ and 1.57℃ at annual, wheat and corn seasonal time scales, respectively. Statistical analysis in Table 2 shows that the increasing trends of annual and seasonal (wheat and corn) temperature were significant at 0.001 level, with slopes of 0.42℃, 0.45℃ and 0.33℃$\cdot$decade^{-1}. Similar increasing trends of temperature were found in southern Spain of about 0.16–0.40℃$\cdot$decade^{-1} (Espadafor *et al.*, 2011), and about 0.2–0.41℃$\cdot$decade^{-1} in France (Chaouche *et al.*, 2010). Chattopadhyay and Hulme (1997) observed an increasing trend in temperature in southern and central India in recent decades in all seasons and over all of India in the post-monsoon season. At global scale, the total temperature increase in the last 100 years (1906–2005) is 0.74℃ (0.56℃ to 0.92℃), with a linear rate of 0.074℃ per decade. Especially in the last 50 years, the linear warming trend (0.13℃ per decade) is nearly twice that for the last 100 years (IPCC, 2007). The warming climate would likely lead to increase potential evapotranspiration and then irrigation amount in less rainfall

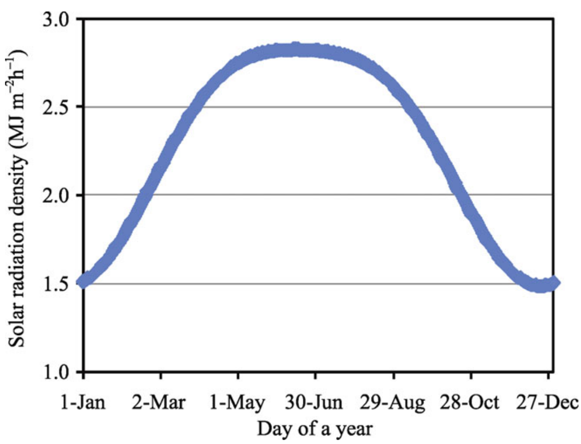

Figure 3 Annual courses of the density of radiation under cloudless condition at the Beijing station

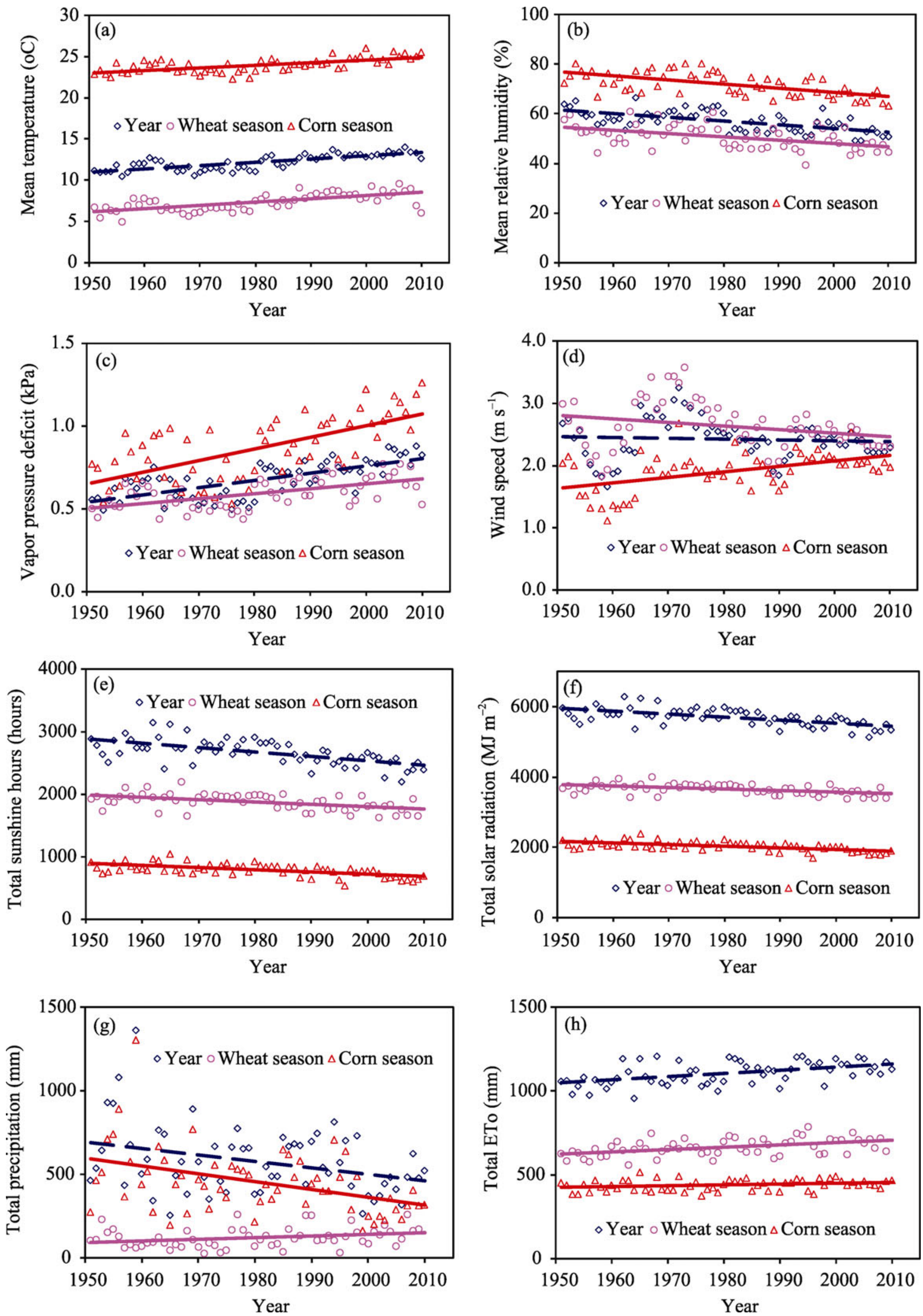

Figure 4 Variations of mean temperature (a), relative humidity (b), vapor pressure deficit (c), wind speed (d), total year sunshine hours (e), total yearly solar radiation (f), total year precipitation (g) and yearly ETo (h) from 1951 to 2010

Table 2 Sen's slope rate of the linear trends of monthly, seasonal and annual mean of each climatic variable and ETo for the period 1951–2010. Asterisks represent the significance level of the trend according to the Mann-Kendall test.

Durations	Items							
	Precipitation	T	RH	VPD	wind	Sunshine hours	Solar radiation	ETo
	mm·year	℃·year	%·year	kPa·year	m·s^{-1}·year	hours/year	MJ·m^{-2}·year	mm·year
Jan	–	0.058*	–0.009	0.001**	–0.014***	–0.397*	–0.319*	0.011
Feb	–	0.079***	–0.189*	0.003***	–0.011**	–0.217	–0.237	0.173**
Mar	0.082*	0.078**	–0.328***	0.005***	–0.007	–0.169	–0.226	0.432***
Apr	0.163+	0.046***	–0.086	0.004**	–0.010+	–0.509*	–0.665*	0.143
May	0.210	0.049*	–0.073	0.004*	0.001	–0.523+	–0.724+	0.139
Jun	0.158	0.026**	–0.066	0.005+	0.003	–1.187***	–1.681***	–0.038
Jul	–1.319*	0.025	–0.208***	0.009***	0.010***	–1.042***	–1.461***	0.151
Aug	–2.179**	0.029*	–0.210***	0.009***	0.011***	–0.782**	–1.057**	0.259**
Sep	–0.226	0.043***	–0.139**	0.005***	0.006*	–0.923***	–1.137***	0.150*
Oct	0.112	0.058***	–0.205***	0.005***	0.002	–0.671**	–0.678**	0.181**
Nov	0.026	0.027*	–0.171**	0.002***	0.005	–0.251	–0.180	0.116**
Dec	–	0.038*	–0.102+	0.002***	–0.006	–0.483*	–0.365*	0.120*
Wheat season Oct. 1 to Jun. 15	0.805+	0.045***	–0.140***	0.003***	–0.009**	–4.251***	–4.635***	1.311**
Corn season Jun. 16 to Sep. 30	–3.877**	0.033***	–0.170***	0.007***	0.008***	–3.486***	–4.683***	0.531*
Annual mean or total	–2.500*	0.042***	–0.147***	0.004***	0.005+	–7.402***	–9.070***	1.951***

Note:
Values without symbol are non-significant.
*** ≤0.001.
** ≤0.01.
* ≤0.05.
+ ≤0.1.

regions (Chattopadhyay and Hulme, 1997).

Similar to the trend of temperature, the annual and crop seasonal mean relative humidity also showed a single trend in the past 60 years, but as shown in Figure 4b this trend showed a decrease. The annual mean RH decreased from 60% in the 1950s to 53% in the 2000s, from 53% to 47% in the wheat season and from 75% to 67% in the corn season. The annual, wheat season and corn season RH decreased significantly (P<0.001) with slopes of 1.5%, 1.4% and 1.7% per decade, respectively. It can be seen there was a greater decrease of RH in the corn season than in the wheat season. Monthly data in Table 2 shows that significant reduction of RH was found from July to November, which results in a greater RH decrease in the corn season. A decreasing relative humidity indicates a greater atmospheric water demand and hence a larger crop water requirement.

Vapor pressure deficit was calculated by air temperature and relative humidity following the methods of Allen *et al*. (1998). It is clearly showed in the calculation method that VPD increases with temperature, and decreases with relative humidity. Figure 4c shows the variations of annual and crop seasonal VPDs in the past 60 years. It can be seen that, both annual and crop seasonal VPDs show increasing trends, which may be mainly due to increasing temperature and decreasing relative humidity (Figures 4a and 4b). Statistical analysis in Table 2 shows that significant increasing trend in VPD was found in all months, with a larger increase from July to October. The increasing rates of annual, wheat seasonal and corn seasonal mean VPDs were 0.04, 0.03 and 0.07 kPa per decade, respectively. Vapor pressure deficit represents the gradient across which water vapor is removed from the evapotranspiring surface into the surrounding air (Allen *et al*., 1998). A greater VPD generally causes a higher evaporation rate. Hence, the increasing VPD in Beijing region will result in an increasing crop evapotranspiration.

The annual mean wind speed varied greatly during the past 60 years (Figure 4d). Clear decreasing trends were found from 1951 to 1959 and from 1972 to 1990, while increasing trends were found in the 1960s and 1990s. During the recent 15 years (1996–2010), the wind speed showed a slight decreasing trend. Statistical analysis for the whole 60-year period in Table 2 shows that, decreasing trends for monthly wind speed were found from December to April with a slope of 0.06–0.14 $m \cdot s^{-1}$ per decade, while increasing trends existed in other months. Hence, wind speed in wheat season was decreasing with years, while it was increasing in corn season. The inverse trends of wind speed between the corn and wheat seasons resulted in an unclear trend of annual wind speed, though the statistical linear slope was 0.05 $m \cdot s^{-1}$ per decade. The variation of wind speed in the wheat season was closer to the annual change than those in the corn season, which may be mainly due to the greater wind speed and longer season (about 8 months) of winter wheat.

Annual total sunshine hours and radiation are illustrated in Figures 4e and 4f, respectively. Both sunshine hours and radiation showed decreasing trends. From the 1950s to 2010s, the annual total sunshine hours and radiation, respectively, decreased by 325 hours and 396 $MJ \cdot m^{-2}$, corresponding to 11.7% and 6.8%, respectively. The linear slopes for annual, wheat and corn seasonal sunshine hours were –74.0, –42.5 and –34.9 hours per decade, respectively, and the corresponding slopes for solar radiation were –90.7, –46.4 and –46.8 $MJ \cdot m^{-2}$ per decade (Table 2). The radiation decrease rate of 90.7 $MJ \cdot m^{-2}$ per decade, equivalent to 0.28 $W \cdot m^{-2}$ per year or 2.1% per decade, is similar to the findings of Stanhill and Cohen (2002). They concluded that at global scale, solar radiation reaching the earth's surface reduced by 0.51–0.05 $W \cdot m^{-2}$ per year or 2.7% per decade. Though radiation decrease in the wheat season (–46.35 $MJ \cdot m^{-2}$ per decade) was close to that in the corn season (–46.83 $MJ \cdot m^{-2}$ per decade) (Table 2), a greater relative reduction rate was found in the corn season. In corn season, total sunshine hours and radiation reduced by 19.3% and 10.3%, respectively, as compared to the corresponding values of 9.4% and 5.4% in the wheat season, mainly due to shorter season duration in corn season (about 3 month and a half) than in wheat season (about 8 month). The greater reduction of sunshine hours and radiation in corn season would possibly inhibit corn growth and yield, because corn biomass linearly increase with cumulative absorbed photosynthetically active radiation (APAR) with a double rate of biomass accumulation per unit APAR as respected to C3 crops like soybean or wheat (Daughtry *et al*., 1992).

Sunshine hours generally depend on cloud cover, manmade aerosols and some air pollutants (including SO_2, NO_x, particulate matter) (Gianna *et al*., 2013; Wang *et al*., 2013). Recent studies pointed out that the most probable cause for the depression of sunshine hours or solar radiation is in the increased concentrations of manmade aerosols and other air pollutants (Stanhill and Cohen, 2001; IPCC, 2007; Liu *et al*., 2010; Gianna *et al*., 2013; Wang *et al*., 2013). These particles can directly attenuate surface solar radiation by scattering and absorbing solar radiation (direct effect) or indirectly attenuate surface solar radiation through their ability to act as cloud condensation nuclei thereby increasing cloud reflectivity and lifetime. All these effects act towards reducing solar radiation with increasing aerosol levels (Wild, 2012; Gianna *et al*., 2013). In Beijing city, vehicular emissions of HC, CO and NOx were estimated to reach 13.33×10^4, 100.02×10^4 and 7.55×10^4 tons, respectively, in 2005 (Wang *et al*., 2009), and vehicle emissions in the urban area made up 75% of the total emissions in Beijing in 2002 for vehicle-related pollutants (DESE, 2005). Temporary transportation control measures, promulgated by the local government of Beijing in 2008 Olympic period, caused the urban traffic emission reductions by more than 50% (Zhou *et al*., 2010). So Li *et al*. (1998) point out that the increasing amount in air turbidity and concentration of air suspended particle caused by city development, including increasing vehicle amount, are the main reasons for the radiation reduction in Beijing city. With an annual increase of 13.4% for vehicle amount in Beijing, radiation will continue decreasing in the future if no air-clear policy will be enforced by the government.

Annual precipitation varied greatly among the years (Figure 4g). The largest precipitation was 1361 mm in 1959, the lowest was 256 mm in 1965, and the annual mean was 577 mm. Precipitation in corn season also varied greatly, which was similar to the behavior of the annual. Compared to the greater variation of annual and corn-seasonal precipitation, its variability in the wheat season was smaller. Figure 4g shows that, corn-seasonal precipitation contributed more to the annual total than the wheat season. The mean annual precipitation in the past 60 years was 577 mm, in which 21% (i.e. 122 mm) was in wheat season, while 79% (i.e. 453 mm) in corn season. Figure 4g further shows that, the annual and corn-seasonal total precipitations were decreasing in the past 60 years, while it was slightly increasing in the wheat seasons. From the 1950s to 2000s, total precipitation in corn season decreased from 553 to 291 mm, while in the wheat season it increased from 118 to 160 mm, which finally resulted in a decreasing annual precipitation from 689 to 448 mm. Table 2 shows that, the decreasing trends for annual and corn-seasonal precipitations were significant ($p<0.05$), with rates of decrease of 25.0 and 38.8 mm per decade, respectively. Trend of increase in the winter season was statistically significant at 0.1 level with a rate of 8.1 mm per decade. It should be noted that in the past decade, there was a sharp reduction of annual and corn-seasonal precipitation. The mean annual and corn-seasonal precipitation averaged over 2001–2010 (referring to as the 2000s) decreased by 120 and 139 mm as compared to those averaged over 1991–2000 (referring to as the 1990s) , accounting for 50% and 53% of total reductions in the past sixty years, respectively. The greater reduction in annual and corn-seasonal precipitation in the past decade caused a serious water shortage in Beijing region. For example annual irrigation amount decreased from 1.74×10^9 to 1.14×10^9 m^3, and groundwater table decreased by approximately one meter per year due to over pumping (Beijing Water Resources Bulletin 2001–2010, Beijing Water Authority). On the other hand, increased precipitation in the wheat season improved wheat growth and reduced irrigation amounts.

Annual total ETo varied from 957 to 1208 mm with a mean of 1105 mm. ETo in winter season contributed mostly to the annual ETo due to the long winter season. The mean ETo in wheat and corn seasons were 665 and 439 mm, respectively. Figure 4a shows that annual and crop-seasonal ETo in the past 60 years increased significantly (Table 2). From the 1950s to 2000s, the annual total ETo increased from 1039 to 1148 mm; wheat seasonal increase was from 620 to 692 mm and corn-seasonal increase was from 423 to 450 mm. The rates of increase were 19.5, 13.1 and 5.3 mm per decade for annual, wheat and corn-seasonal ETo, respectively (Table 2). Similar increase rates ranging 0.005–0.01 mm per day of ETo, equivalent to 18–35 mm per decade, were found in Southern Spain by Espadafor *et al*. (2011). While in most China, the seasonal and annual ETos show decline tendencies during the past 50 years (Gao *et al*., 2006; Tang *et al*., 2011; Huo *et al*., 2013). The variation of ETo trend in different regions may be due to the changes of dominated meteorological factors (Gao *et al*., 2006; Gong *et al*., 2006; Huo *et al*., 2013).

Increased ETo indicates an increased potential for crop evapotranspiration. Considering the decreased precipitation, especially in corn season, water requirement for irrigation would be obviously increasing during the past 60 years in Beijing region.

3.3 Sensitivity analysis of ETo to the change of climatic variables

The climatic variables considered in this study showed increasing or decreasing trends during the past 60 years. The influence of each variable on ETo was estimated using the sensitivity analysis method described in Section 2.3.2. The sensitivity analysis was done at monthly, seasonal (wheat and corn) and annual scales. For the monthly scale, the mean, maximum and minimum daily temperature, and daily mean relative humidity, wind speed and sunshine hours were averaged in each month. To smooth abrupt climatic changes on ETo, a ten-year mean data was used. The daily mean climatic variables in each month were averaged from 1951 to 1960 (referring to as the 1950s) and from 2001 to 2010 (referring to as the 2000s). For the sensitivity analysis, the mean daily values in the 1950s were set as reference data. The effect of the change of each variable on ETo in the past 60 years was studied by replacing this variable using the corresponding one in the 2000s leaving the other variables in their reference values in the 1950s. The results of the sensitivity analysis are listed in Table 3.

It can be seen in Table 3 that, increases of daily Tmax and Tmin from the 1950s to 2000s resulted in small ETo reduction, less than 0.02 mm·day^{-1} or 1% in the past 60 years. Tmax and Tmin are positively related to the rate of long-wave energy emission as shown in Eqn (5). The increases in Tmax and Tmin indicate larger long-wave energy emission, which results in a reduction of net radiation, hence decreasing ETo as shown by Eqn (1). Increasing air temperature resulted in a greater increase of ETo as shown in Table 3. As compared to the mean daily ETo in each month in the 1950s, the increment of ETo due to air temperature change in the 2000s ranges from 0.08 to 0.34 mm·day^{-1} with a mean increment rate of 0.20 mm·day^{-1}. The largest increments were found in March, April and May with values higher than 0.30 mm·day^{-1}, and the lowest increments were from October to January with values less than 0.15 mm·day^{-1}. In the wheat season, the mean increment of daily ETo caused by increasing temperature was 0.217 mm·day^{-1}, and was close to that (0.193 mm·day^{-1}) in the corn season.

Table 3 Sensitivity analysis of climatic changes on ETo

	T_{mean}		T_{max}		T_{min}		RH		Wind		Sunshine hours		ETo	
	ETo Change amount mm·day	%	ETo change amount mm·day	%	ETo change amount mm·day	%	ETo change amount mm·day	%	ETo change amount mm·day	%	ETo change amount mm·day	%	Change amount	%
Jan	0.136	14.0	–0.004	–0.4	–0.009	–0.9	0.043	4.4	–0.076	–7.9	0.003	0.3	0.081	8.3
Feb	0.223	16.9	–0.008	–0.6	–0.010	–0.8	0.091	6.9	–0.038	–2.9	–0.009	–0.7	0.245	18.6
Mar	0.340	16.7	–0.013	–0.6	–0.011	–0.6	0.368	18.1	0.031	1.5	0.009	0.5	0.807	39.7
Apr	0.309	7.6	–0.005	–0.1	–0.015	–0.4	0.083	2.1	–0.059	–1.4	–0.093	–2.3	0.207	5.1
May	0.305	6.2	–0.007	–0.1	–0.015	–0.3	0.119	2.4	0.067	1.4	–0.084	–1.7	0.403	8.2
Jun	0.201	4.0	–0.003	–0.1	–0.011	–0.2	0.172	3.4	0.111	2.2	–0.003	–0.1	0.183	3.6
Jul	0.167	3.8	–0.004	–0.1	–0.006	–0.1	0.234	5.4	0.092	2.1	–0.340	–7.8	0.293	6.7
Aug	0.191	5.1	–0.005	–0.1	–0.007	–0.2	0.230	6.1	0.071	1.9	–0.172	–4.6	0.457	12.2
Sep	0.233	7.4	–0.006	–0.2	–0.015	–0.5	0.158	5.0	0.066	2.1	–0.006	–0.2	0.286	9.1
Oct	0.139	7.0	–0.003	–0.2	–0.011	–0.5	0.185	9.3	0.013	0.6	–0.048	–2.4	0.290	14.6
Nov	0.090	7.5	–0.004	–0.3	–0.006	–0.5	0.138	11.5	0.008	0.7	0.000	0.0	0.238	19.8
Dec	0.080	8.7	–0.002	–0.2	–0.007	–0.8	0.091	9.9	0.028	3.1	0.006	0.7	0.212	23.1
Wheat season	0.217	8.6	–0.005	–0.2	–0.011	–0.4	0.135	5.4	0.007	0.3	–0.045	–1.8	0.308	12.3
Corn season	0.193	4.5	–0.004	–0.1	–0.008	–0.2	0.204	4.7	0.080	1.9	–0.298	–6.9	0.258	6.0
Annual	0.253	7.4	–0.005	–0.2	–0.010	–0.3	0.187	5.5	0.023	0.7	–0.104	–3.1	0.365	10.7

Note: "ETo change amount" in each column is the difference of reference daily ETo in the 1950s and that calculated using the value of the corresponding variable in the 2000s while the other variables are those in the 1950s. "Change amount" in the ETo column indicates the ETo difference between the 1950s and 2000s. "%" means the changed percentage caused by each variable's change in the given period.

The decreasing RH during the past 60 years caused ETo increase in each month and season. The largest increment of daily ETo caused by RH was 0.368 mm·day^{-1} found in March, values between 0.20 and 0.30 mm·day^{-1} were found in July and August, and values less than 0.10 mm·day^{-1} were from December to February. Relative humidity decrease in the corn season caused a greater increase of ETo (0.204 mm·day^{-1}) as compared to those (0.135 mm·day^{-1}) in the wheat season.

Changes of wind speed in the past 60 years have caused daily ETo increases with rates of 0.007, 0.08 and 0.023 mm·day^{-1} in wheat season, corn season and on an annual base, respectively. However, it should be noted that wind changes in January, February and April resulted in a reduction of ETo, as compared to the increases in other months.

Reductions of sunshine hours in the past 60 years caused ETo decreases in most of the months. The greatest decrease of daily ETo caused by sunshine hours was –0.350 mm·day^{-1}, in July, followed by –0.172 mm·day^{-1} in August. The decreasing rates in other months were generally less than 0.1 mm·day^{-1}. The larger decreasing amounts in July and August contributed to a higher reduction rate of 0.298 mm·day^{-1} in the corn season as compared to that in the wheat season.

Mean daily ETo of each month caused by the change in climatic variables increased by 4% to 40% during the past 60 years. The largest change of daily ETo was 0.807 mm·day^{-1} in March, followed by May and August, whose increments were 0.403 and 0.457 mm·day^{-1}, respectively. In half of the 12 months, the daily ETo increment was in the range of 0.20–0.30 mm·day^{-1}. The least increment was 0.081 mm·day^{-1}, found in January. In the past 60 years, mean daily ETo increased by 0.308 and 0.258 mm·day^{-1}, or 1.31 and 0.53 mm per season in wheat and corn seasons, respectively. The mean daily ETo increased by 0.365 mm·day^{-1} or 1.95 mm per year on a yearly base. This yearly increment was close to the value of 1.3 mm·year^{-1} found in this region by Tang *et al*. (2011).

Among the six climatic variables, mean temperature and relative humidity were the first two key factors for ETo increase in the past 60 years, causing daily ETo increases by 7.4% and 5.7% on an annual base, respectively. The third factor was sunshine hours, which caused daily ETo reduction by 3.1%. Wind speed, maximum and minimum temperatures had minor effects on ETo change in the past 60 years.

Generally, the sensitivity of ETo to meteorological variables varies with the climatic characteristics in each of the study regions. Tang *et al*. (2011) found in the Haihe River Basin of North China, a region near Beijing in this study, that, ETo is most sensitive to temperature and radiation they changed ETo by 2.5 and –1.2 mm·year^{-1}, respectively. This finding is in agreement with the results presented in this study. While in the arid region of Northwest China, wind speed was the most sensitive meteorological variable, followed by relative humidity, temperature and radiation (Huo *et al*., 2013). The greater effect of wind speed on ETo in Northwest China can be explained by the lower amount of water vapor carried by the wind in drier climates as compared to the higher humidity of the wind flow in relative humid climates, like in this study region. In general, it should be noted that mostly temperature and sunshine duration are the key factors for ETo changes (Goyal, 2004; Tanaka *et al*., 2009; Liang *et al*., 2010; Tang *et al*., 2011; Espadafor *et al*., 2011; Tabari *et al*., 2011; Chen *et al*., 2012). The reason may be due that the two climatic variables changed greatly in the past few centuries. Global air temperature during 1906–2005 increased by 0.74 ℃ (0.56–0.92℃) from t observations (IPCC, 2007), and the continued greenhouse gas emissions at or above current rates would cause further warming during the 21st century (IPCC, 2007). A clear declining trend of surface solar radiation (3–9 W·m^{-2}) has been found in China, India, and other regions (Wild *et al*., 2009), especially in some megacities like Shanghai, China (Xu *et al*., 2011). The main cause is the obvious increasing of aerosols and pollutants (de Meij *et al*., 2012), because they greatly change the optical properties of the atmosphere, in particular those of clouds, thereby attenuate surface solar radiation (Stanhill and Cohen, 2001; Wild, 2012).

The gradient of climatic variable effect on ETo in the wheat season was different from that in corn season. In the wheat season, ETo has decreased by 12.3%, mainly because of mean temperature (8.6%) and relative humidity (5.4%). However, in the corn season, sunshine hours, relative humidity and temperature caused ETo changes by –6.9%, 4.7% and 4.5%, respectively. On a monthly base, climatic variables played different roles in ETo change. Under most months, mean temperature played the first important role for ETo change, followed by relative humidity, sunshine hours and wind speed, and the less important factors were maximum and minimum temperatures, which was similar to the order of importance on a yearly base. But in some months, the key factors for ETo change were different. For example, in March, August, October, November and December, the first important factor was relative humidity, which caused ETo increase by 18.1%, 6.1%, 9.3%, 11.5 and 9.9%, respectively. The first key factor in July was sunshine hours, which caused a reduction of ETo by 7.8%. This may conclude that the effects of the main climatic variables (temperature, relative humidity, wind speed and radiation) to ETo depends on the climatic region and periods.

4 Conclusions

(1) The changing trends of the climatic meteorological variables in Beijing in the past 60 years are: increase of air temperature, gradual decrease of relative humidity and sunshine hours, wind speed waved greatly without a significant trend. Saturated vapor pressure deficit increased during the past 60 years, mainly due to temperature increase and RH decrease. All these variations caused an overall increase in estimated ETo during the past 60 years with a rate of 1.95 $mm \cdot year^{-1}$.

(2) Sensitivity analysis showed that: mean air temperature and relative humidity in the past 60 years have caused ETo increases by 7.4% and 5.5% on a yearly base, respectively; sunshine hours increase caused ETo decrease by 3.1%; wind speed, and maximum and minimum temperatures variations had minor effect on ETo change during the past 60 years. In wheat season, ETo has been decreased by 12.3%, mainly because of mean temperature (8.6%) and relative humidity (5.4%) changes. But in the corn season, sunshine hours, relative humidity and temperature caused ETo changes by –6.9%, 4.7% and 4.5%, respectively.

Acknowledgement

The authors greatly appreciate the China Meteorological Data Sharing Service System (http://cdc.cma.gov.cn/) for providing valuable meteorological data, the editor and the anonymous reviewers for their helpful suggestions on this paper.

References

Allen R G, Perreira L S, Raes D *et al*., 1998. Crop Evapotranspiration: Guidelines for Computing Crop Water Requirements, FAO Irrigation and Drainage Paper No.56. FAO, Rome.

Bates B C, Kundzewicz Z W, Wu S *et al*., 2008: Climate Change and Water. Technical Paper of the Intergovernmental Panel on Climate Change, IPCC Secretariat, Geneva, 210 pp.

Chaouche K, Neppel L, Dieulin C *et al*., 2010. Analyses of precipitation, temperature and evapotranspiration in a French Mediterranean region in the context of climate change. *Comptes Rendus Geosciences*, 342(3): 234–243.

Chattopadhyay N, Hulme M, 1997. Evaporation and potential evapotranspiration in India under conditions of recent and future climate change. *Agricultural and Forest Meteorology*, 87: 55–73.

Chen X, Li B L, Li Q *et al*., 2012. Spatio-temporal pattern and changes of evapotranspiration in arid Central Asia and Xinjiang of China. *Journal of Arid Land*, 4(1): 105-112.

de Meij A, Pozzer A, Lelieveld J, 2012. Trend analysis in aerosol optical depths and pollutant emission estimates between 2000 and 2009. *Atmospheric Environment*, 51: 75–85.

Daughtry C S T, Gallo K P, Goward S N *et al*., 1992. Spectral estimates of absorbed radiation and phytomass production in corn and soybean canopies. *Remote Sensing of Environment*, 39(2): 141–152.

Department of Environmental Science and Engineering, Tsinghua University (DESE). Mobile source database, emission inventory and treatment proposal for Beijing, H030630540430. Beijing, China: Tsinghua University, 2005.

Espadafor M, Lorite I J, Gavilán P *et al*., 2011. An analysis of the tendency of reference evapotranspiration estimates and other climate variables during the last 45 years in Southern Spain. *Agricultural Water Management*, 98: 1045–1061.

Gao G, Chen D, Ren G *et al*., 2006. Spatial and temporal variations and controlling factors of potential evapotranspiration in China: 1956–2000. *Journal of Geographical Sciences*, 16(1): 3–12.

Gianna K, Georgia P, Athanasios P *et al*., 2013. Dimming/brightening in Athens: Trends in sunshine duration, cloud cover and reference evapotranspiration. *Water Resource Management*, 27: 1623–1633.

Gong L B, Xu C Y, Chen D L *et al*., 2006. Sensitivity of the Penman-Monteith reference evapotranspiration to key climatic variables in the Changiiang (Yangtze River) basin. *Journal of Hydrology*, 329(3/4): 620–629.

Goyal R K, 2004. Sensitivity of evapotranspiration to global warming: A case study of arid zone of Rajasthan (India). *Agricultural Water Management*, 69: 1–11.

Hamed K H, 2008. Trend detection in hydrologic data: The Mann–Kendall trend test under the scaling hypothesis. *Journal of Hydrology*, 349: 350–363.

Haskett J D, Pachepsky Y A, Acock B, 2000. Effect of climate and atmospheric change on soybean water stress: A study of Iowa. *Ecological Modelling*, 135(2/3, 5): 265–277.

Huntington T G, 2006. Evidence for intensification of the global water cycle: Review and synthesis. *Journal of Hydrology*, 319(1–4): 83–95.

Huo Z L, Dai X Q, Feng S Y *et al*., 2013. Effect of climate change on reference evapotranspiration and aridity index in arid region of China. *Journal of Hydrology*, 492: 24–34.

IPCC, 2007. Climate Change 2007: Synthesis Report. An Assessment of Intergovernmental Panel on Climate Change. Geneva, Switzerland, http://ipcc.ch/index.html.

Li X W, Li W L, Zhou X J, 1998. Analysis of the solar radiation variation of China in recent 30 years. *Quarterly Journal of Applied Meteorology*, 9(1): 24–31. (in Chinese)

Liang L Q, Li L J, Liu Q, 2010. Temporal variation of reference evapotranspiration during 1961–2005 in the Taoer River basin of Northeast China. *Agricultural and Forest Meteorology*, 150: 298–306.

Liang L Q, Li L J, Zhang L *et al*., 2008. Sensitivity of the reference crop evapotranspiration in growing season in the West Songnen Plain. *Transaction of Chinese Society of Agricultural Engineering*, 24(5): 1–5. (in Chinese)

Liang L Q, Yan M H, Deng W *et al*., 2006. Change of reference crop evapotranspiration from West Songnen Plain. *Progress in Geography*, 25(3): 22–31. (in Chinese)

Liu B, Hu Q, Wang W C *et al*., 2011. Variation of actual evapotranspiration and its impact on regional water resources in the Upper Reaches of the Yangtze River. *Quaternary International*, 244(2): 185–193.

Liu C, Zhang D, Liu X *et al*., 2012. Spatial and temporal change in the potential evapotranspiration sensitivity to meteorological factors in China (1960−2007). *Journal of Geographical Sciences*, 22(1): 3–14.

Liu C, Zhang X, Zhang Y, 2002. Determination of daily evaporation and evapotranspiration of winter wheat and maize by large-scale weighing lysimeter and micro-lysimeter. *Agricultural and Forest Meteorology*, 111: 109–120.

Liu H J, Kang Y H, 2007. Sprinkler irrigation scheduling of winter wheat in the North China Plain using a 20 cm standard pan. *Irrigation Science*, 25 (2): 149–159.

Liu H J, Yu L P, LuoY *et al*., 2011. Responses of winter wheat (*Triticum aestivum* L.) evapotranspiration and yield to sprinkler irrigation regimes. *Agricultural Water Management*, 98: 483–492.

Liu M, Shen Y, Zeng Y *et al*., 2010. Trend in pan evaporation and its attribution over the past 50 years in China. *Journal of Geographical Sciences*, 20(4): 557–568

Liu Q, Yang Z, 2010. Quantitative estimation of the impact of climate change on actual evapotranspiration in the

Yellow River Basin, China. *Journal of Hydrology*, 395: 226–234.

Möller M, Tanny J, Li Y *et al*., 2004. Measuring and predicting evapotranspiration in an insect-proof screenhouse. *Agricultural and Forest Meteorology*, 127: 35–51.

Salmi T, Määttä A, Anttila P *et al*., 2002. Detecting trends of annual values of atmospheric pollutants by the Mann-Kendall test and Sen's slope estimates: The Excel template application MAKESENS. Finnish Meteorological Institute, Helsinki, Finland.

Sen P K, 1968. Estimates of the regression coefficient based on Kendall's Tau. *Journal of American Statistical Association*, 63: 1379–1389.

Stanhill G, Cohen S, 2001. Global dimming: a review of the evidence for a widespread and significant reduction in global radiation with discussion of its probable causes and possible agricultural consequences. *Agricultural and Forest Meteorology*, 107(4): 255–278.

Tabari H, Marofi S, Aeini A *et al.*, 2011. Trend analysis of reference evapotranspiration in the western half of Iran. *Agricultural and Forest Meteorology*, 151: 128–136.

Tanaka N, Kume T, Yoshifuji N *et al*., 2008. A review of evapotranspiration estimates from tropical forests in Thailand and adjacent regions. *Agricultural and Forest Meteorology*, 148: 807–819.

Tang B, Tong L, Kang S Z *et al*., 2011. Impacts of climate variability on reference evapotranspiration over 58 years in the Haihe River Basin of North China. *Agricultural Water Management*, 98: 1660–1670.

Tao F, Yokozawa M, Hayashi Y *et al*., 2003. Future climate change, the agricultural water cycle, and agricultural production in China. *Agriculture Ecosystems and Environment*, 95: 203–215.

Thomas A, 2000. Climatic changes in yield index and soil water deficit trends in China. *Agricultural and Forest Meteorology*, 102: 71–81.

Wang H, Fu L, Lin X *et al*., 2009. A bottom-up methodology to estimate vehicle emissions for the Beijing urban area. *Science of the Total Environment*, 407: 1947–1953.

Wang Y, Yang Y, Han S *et al*., 2013. Sunshine dimming and brightening in Chinese cities (1955–2011) was driven by air pollution rather than clouds. *Climate Research*, 56: 11–20.

Wang Y J, Jiang T, Bothe O, 2007. Changes of pan evaporation and evapotranspiration in the Yangtze River basin. *Theoretical and Applied Climatology*, 90: 13–23.

Wild M, 2009. Global dimming and brightening: A review. *Journal of Geophysical Research*, 114, D00D16, doi: 10.1029/2008JD011470.

Wild M, 2012. Enlightening global dimming and brightening. *Bulletin of the American. Meteorological Society*, 93: 27–37.

Xu J, Li C, Shi H *et al*., 2011. Analysis on the impact of aerosol optical depth on surface solar radiation in the Shanghai megacity, China. *Atmospheric Chemistry and. Physics*, 11: 3281–3289.

Yang J, McBridea J, Zhou J *et al.*, 2005. The urban forest in Beijing and its role in air pollution reduction. *Urban Forestry and Urban Greening*, 3: 65–78.

Yue N, 2007. The characteristics of water resource and sustainable utilization in Beijing. *Journal of Capital Normal University* (*Natural Science Edition*), 28 (3): 107–113. (in Chinese)

Zhang X, Chen S, Sun H *et al*., 2011. Changes in evapotranspiration over irrigated winter wheat and maize in North China Plain over three decades. *Agricultural Water Management*, 98: 1097–1104.

Zhou Y, Wu Y, Yang L *et al*., 2010. The impact of transportation control measures on emission reductions during the 2008 Olympic Games in Beijing, China. *Atmospheric Environment*, 44: 285–293.